STEM CELLS®

CANCER STEM CELLS

DNER, an Epigenetically Modulated Gene, Regulates Glioblastoma-Derived Neurosphere Cell Differentiation and Tumor Propagation

PENG SUN,[a] SHULI XIA,[a] BACHCHU LAL,[a] CHARLES G. EBERHART,[b] ALFREDO QUINONES-HINOJOSA,[c] JAREK MACIACZYK,[e] WILLIAM MATSUI,[d] FRANCESCO DIMECO,[f] SARA M. PICCIRILLO,[g] ANGELO L. VESCOVI,[g] JOHN LATERRA[a]

[a]Department of Neurology, The Johns Hopkins University School of Medicine and The Hugo W. Moser Research Institute at Kennedy Krieger, Baltimore, Maryland, USA; Departments of [b]Pathology, [c]Neurosurgery, and [d]Oncology, The Johns Hopkins School of Medicine, Baltimore, Maryland, USA; [e]Department of General Neurosurgery and Laboratory of Molecular Neurosurgery, University of Freiburg, Freiburg, Germany; [f]Department of Neurosurgery, Instituto Nazionale Neurologico "Carlo Besta," Milan, Italy; [g]Department of Biotechnology and Biosciences, University of Milan Bicocca, Milan, Italy

Key Words. Histone acetylation • Glioma • Stem cell • Oncosphere

ABSTRACT

Neurospheres derived from glioblastoma (GBM) and other solid malignancies contain neoplastic stem-like cells that efficiently propagate tumor growth and resist cytotoxic therapeutics. The primary objective of this study was to use histone-modifying agents to elucidate mechanisms by which the phenotype and tumor-promoting capacity of GBM-derived neoplastic stem-like cells are regulated. Using established GBM-derived neurosphere lines and low passage primary GBM-derived neurospheres, we show that histone deacetylase (HDAC) inhibitors inhibit growth, induce differentiation, and induce apoptosis of neoplastic neurosphere cells. A specific gene product induced by HDAC inhibition, Delta/Notch-like epidermal growth factor-related receptor (DNER), inhibited the growth of GBM-derived neurospheres, induced their differentiation in vivo and in vitro, and inhibited their engraftment and growth as tumor xenografts. The differentiating and tumor suppressive effects of DNER, a noncanonical Notch ligand, contrast with the previously established tumor-promoting effects of canonical Notch signaling in brain cancer stem-like cells. Our findings are the first to implicate noncanonical Notch signaling in the regulation of neoplastic stem-like cells and suggest novel neoplastic stem cell targeting treatment strategies for GBM and potentially other solid malignancies. STEM CELLS *2009;27:1473–1486*

Disclosure of potential conflicts of interest is found at the end of this article.

INTRODUCTION

During the past decade, there has been a re-emergence of the concept that cancers harbor small populations of malignant stem-like cells that sustain tumor growth and recurrence. These "neoplastic stem cells" [1], which share the defining phenotypic characteristics of self-renewal, multipotential differentiation at least equivalent to that in the primary tumor, and long-term tumor propagation [2, 3], have been identified in leukemia and multiple myeloma [4–6], and more recently in solid tumors, including mammary carcinoma [7] and primary brain tumors [3, 8–10]. The potential role for multipotent stem/progenitor cells in brain cancer initiation is supported by the fact that directing oncogenic growth signals to nestin-positive or glial fibrillary acidic protein $(GFAP)^+$ neural progenitor cells in rodents causes high-grade glioma [11, 12]. Independent of the potential contribution of stem cells to tumor initiation, a current view is that neoplastic cells with stem-like properties underpin the maintenance and therapeutic resistance of malignant glioma. This concept is based on the identification of tumor cells that express stem cell markers (CD133, aldehyde dehydrogenase [ALDH], side-population), grow in vitro as neurospheres under serum-free conditions that support the growth of normal neural stem cells, resist ionizing radiation, and propagate tumor xenografts with high

Author contributions: P.S.: conception and design, collection/assembly of data, data analysis/interpretation, manuscript writing, final approval; S.X.: collection/assembly of data, data analysis/interpretation, final approval; B.L.: collection/assembly of data, data analysis/interpretation, final approval; C.E.: conception and design, final approval; A.Q.: provision of study material, final approval; J.M.: provision of study material, final approval; W.M.: collection/assembly of data, final approval; F.D.: provision of study material, final approval; S.P.: provision of study material, final approval; A.V.: provision of study material, final approval; J.L.: conception and design, collection/assembly of data, data analysis/interpretation, manuscript writing, final approval.

Correspondence: John Laterra, M.D., Ph.D., The Hugo W. Moser Research Institute at Kennedy Krieger, 707 N. Broadway, Baltimore, Maryland 21205, USA. Telephone: 443-923-2679; Fax: 443-923-2695; e-mail: laterra@kennedykrieger.org Received October 14, 2008; accepted for publication April 1, 2009; first published online in STEM CELLS *EXPRESS* April 9, 2009. 1066-5099/2009/$30.00/0 doi: 10.1002/stem.89

efficiency [3, 8–10, 13–15]. Understanding the molecular mechanisms that regulate the stem-like tumorigenic phenotype of these cells will improve our understanding of malignant brain tumors and lead to novel stem cell-targeting therapeutics [16–18].

Epigenetic mechanisms of gene expression regulation play an important role in the oncogenic phenotype and in the maintenance/differentiation of normal neural stem cells [19–21]. One of the most prominent of these epigenetic mechanisms involves chromosome modification by histone acetylation, which is determined by the opposing actions of histone acetyltransferases and histone deacetylases (HDACs) [22, 23]. Acetylation of lysine residues in the histone tail promotes gene transcription by relaxing the chromosome, allowing the transcriptional machinery to access DNA. Conversely, histone deacetylation often followed by methylation compacts chromatin and represses gene expression [24]. Neural stem cell proliferation can be regulated by histone acetylation/deacetylation via numerous molecular mechanisms, including cell cycle regulation, apoptosis control, and the activation of differentiation [20, 25–27]. Oncogenesis is associated with a relative decrease in histone acetylation, leading to the transcriptional repression of tumor suppressor genes, a common event contributing to tumor formation [28].

In light of the accelerating interface between brain cancer and neural stem cells and the sensitivity of both to histone modification, we used HDAC inhibitors (HDACIs) to explore the biological and molecular basis of the glioblastoma (GBM) stem-like cell phenotype. HDACIs were found to inhibit the growth of GBM-derived neurospheres, induce neurosphere cell apoptosis, and deplete neurosphere cultures of cells expressing stem cell markers. HDACIs induced GBM-derived neurosphere cell differentiation and inhibited the ability of neurosphere cells to propagate tumor xenografts. Biological responses to HDAC inhibition were mediated, in part, by upregulating the noncanonical Notch ligand Delta/Notch-like epidermal growth factor (EGF)-related receptor (DNER), which was found to inhibit GBM-derived neurosphere formation, induce neurosphere cell differentiation, and inhibit the growth of neurosphere-derived tumor xenografts. This is the first evidence that the DNER signaling pathway has differentiating and tumor-suppressing actions on glioma-derived stem-like cells.

Experimental Procedures

Reagents

All reagents were purchased from Sigma Chemical Co. (St. Louis, http://www.sigmaaldrich.com) unless stated otherwise. Trichostatin A (TSA) and MS-275 (*N*-(2-aminophenyl)-4-[*N*-(3-pyridineyl-methoxycarbonyl)aminomethyl]-benzamide) were prepared as stock solutions in dimethylsulfoxide (DMSO). In all the experiments, the final DMSO concentration was $<0.1\%$.

Cell Culture

The human GBM-derived neurosphere lines HSR-GBM1A (20913), HSR-GBM 1B (10627), and 050,509 were derived by Vescovi and colleagues and maintained in serum-free medium supplemented with EGF and fibroblast growth factor (neurosphere medium), as previously described [10, 29, 30]. The DM140207 neurosphere line was derived from a GBM at the University of Freiburg and primary JHH225 neurospheres were derived from a malignant glioma at Johns Hopkins University (Baltimore, Maryland) using the same methods and culture conditions. JHH225 neurospheres were used at passage ≤ 9. All human materials were obtained and used in compliance with the Johns Hopkins institutional review board.

Cell Growth and Clonogenic Assays

Cell growth was measured by colorimetric assay using 3-(4,5-dimethylthiazol-2-yl)-5(3-carboxymethonyphenol)-2-(4-sulfophenyl)-2H-tetrazolium (MTS) (Promega, Madison, WI, http://www.promega.com). Briefly, 50 μl of a stock solution of MTS was added to each cell culture well to achieve a final concentration of 333 μg/ml. The reduction in MTS, reflecting the number of viable cells per well, was measured after 3 hours by quantifying the absorbance at 490 nm.

For soft agar clonogenic assays, agarose (1%; Invitrogen, Carlsbad, CA, http://www.invitrogen.com) in Dulbecco's modified Eagle's medium was cast on the bottom of plastic six-well plates. Dissociated neurosphere cells were suspended in neurosphere culture medium containing 0.5% agarose equilibrated at 37°C and plated at 5×10^3 cells per well above a bottom layer of 1% agarose. Cells were incubated in a humidified incubator containing 5% CO_2 and 95% air at 37°C for 2 hours and then the medium was replaced with that containing 200 nM TSA. Cultures were incubated in 5% CO_2 and 95% air at 37°C for 14 days and then colony formation was scored by measuring the number of spheres ≥ 100 μm in diameter in nine random microscopic fields per well.

Transient Transfection

Neurosphere cells were transfected with hemagglutinin-tagged full-length DNER expression plasmid, a kind gift of Mineko Kengaku (RIKEN Brain Science Institute, Saitama, Japan) [31], using Amaxa nucleofection technology (Amaxa, Koeln, Germany, http://www.amaxa.com). Cells were suspended in Amaxa Primary Neurons Kit solution, according to Amaxa guidelines. Briefly, a 100-μl suspension of 2-5 $\times$ 10^6 cells was mixed with 3 μg plasmid DNA and subjected to nucleofection using an Amaxa Nucleofector apparatus. Cells were then immediately transferred into six- or 12-well tissue culture plates containing neurosphere culture medium prewarmed to 37°C. Cells were cultured for an additional $\sim$72 hours before experimental analyses. Transfection efficiencies were routinely $\sim$60% as measured by parallel transfection with a green fluorescent protein reporter under identical conditions.

Immunoblot Analysis

SDS-PAGE was performed on 30 μg of cellular protein per lane using 4%–20% gradient Tris-glycine gels according to the method of Towbin et al. with some modifications [32, 33]. Proteins were electrophoretically transferred to nitrocellulose membranes (GE Healthcare, San Diego, http://www.gehealthcare.com). Membranes, except for those to be probed with anti-DNER, were incubated for 1 hour in Odyssey Licor Blocking Buffer (LI-COR Biosciences, Lincoln, NE, http://www.licor.com) at room temperature and then overnight with anti-glyceraldehyde-3-phosphate dehydrogenase (1:7,500; Santa Cruz Biotechnology Inc., Santa Cruz, CA, http://www.scbt.com) or anti-β-actin (1:6,000; Sigma), anti-Deltex-1 (1:300; Santa Cruz Biotechnology), anti-GFAP (1:500; Dako, Carpinteria, CA, http://www.dakousa.com), anti-TuJ1 (1:1,000; Millipore Corporation, Billerica, MA, http://www.millipore.com), anti-histone-4 (1:1,500; Upstate, Charlottesville, VA, http://www.upstate.com), or anti-scetyl-histone-4 (1:1,000; Upstate) at 4°C in Odyssey Blocking Buffer (LI-COR Biosciences). After rinsing, membranes were incubated with IRDye secondary antibodies (1:15,000; LI-COR Biosciences) and protein expression changes were quantified by dual wavelength immunofluorescence Odyssey Infrared

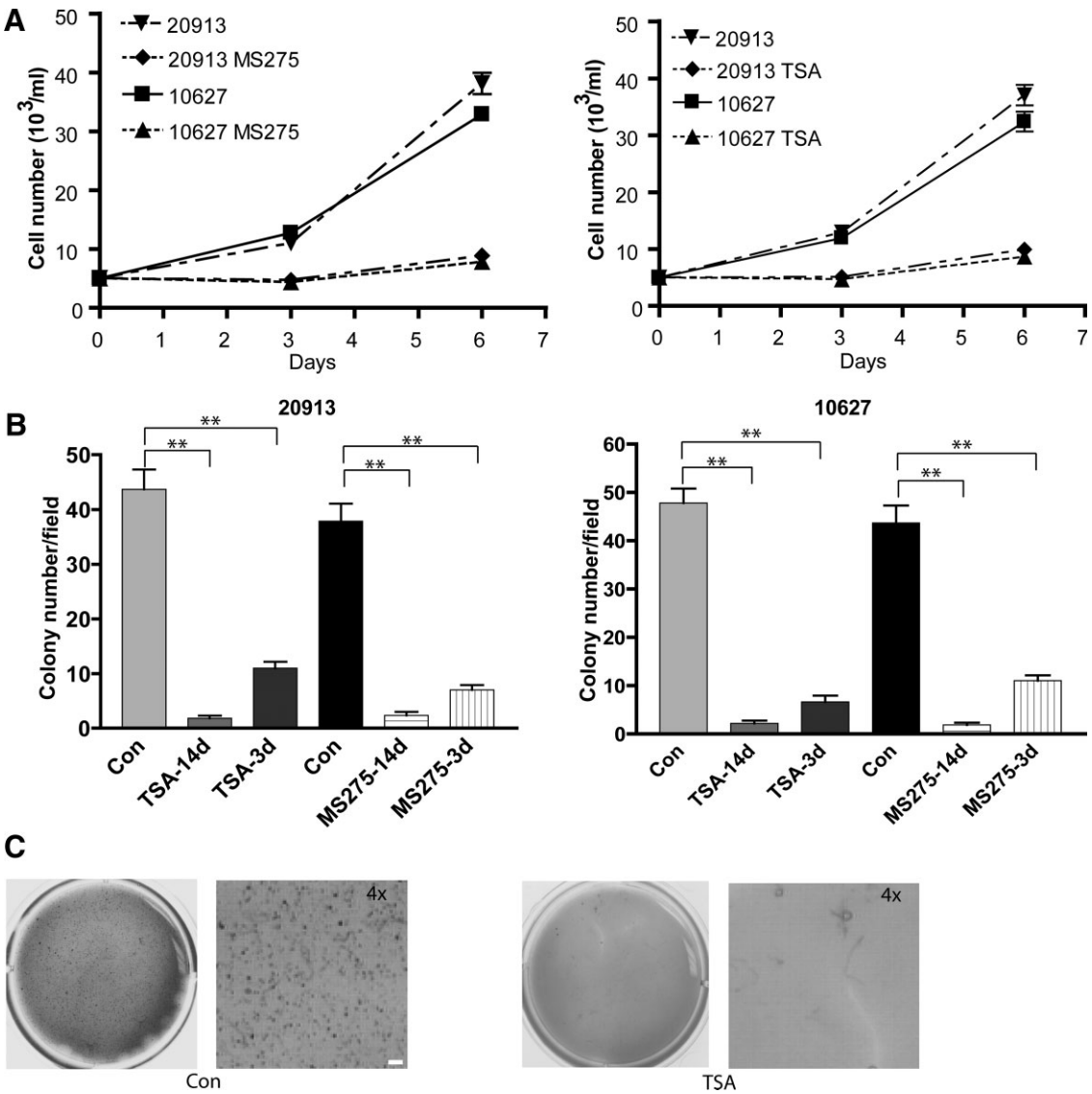

Figure 1. Growth inhibition of GBM-derived neurospheres by HDAC inhibitors. **(A):** GBM-derived neurosphere lines 20913 and 10627 were incubated with TSA (200 nM) or MS-275 (4 nM) for 6 days. Neurosphere cell growth was decreased ~80% by HDAC inhibition. **(B):** GBM-derived neurospheres were cultured continuously for 14 days in neurosphere medium either with buffer only (Con) or with TSA (200 nM) or MS-275 (4 μM). Alternatively, neurospheres were treated transiently with TSA (or MS-275) for only 3 days and then transferred to drug-free neurosphere medium for 11 additional days. Neurospheres were then immobilized in agar and the number of neurospheres measuring >100 μm diameter per low powered microscopic field was counted by computer-assisted morphometry. Neurospheres treated with either TSA or MS-275 for either 3 days or 14 days differed statistically significantly from controls. $^{**}p < .01$. **(C):** Shown are representative agar plates (3.5 cm diameter) and 4× microscopic fields (bar = 100 μm) of neurospheres treated with TSA for 14 days as described in **(B)**. Data are shown as the mean ± standard error of the mean. Abbreviations: Con, control; GBM, glioblastoma; HDAC, histone deacetylase; TSA, trichostatin A.

Imaging System (LI-COR Biosciences) scanning of the membranes. Immunoblots probed with anti-DNER (1:500; Abnova Corporation, Taipei City, Taiwan, http://www.abnova.com) utilized peroxidase-conjugated secondary antibodies, essentially as previous described [34].

Quantitative Real-Time Polymerase Chain Reaction

Total cellular RNA was extracted using the RNeasy Mini kit (Qiagen, Inc., Chatsworth, CA, http://www1.qiagen.com) and purified using RNeasy columns according to the manufacturer's instructions. The purity and amount of total RNA were spectrophotometrically estimated by measuring absorbance at 260 nm and 280 nm. The integrity of rRNA was checked using agarose gel electrophoresis. Total RNA (1 μg) was reverse-transcribed (RT) using the oligo(dT)12-18 primer and Superscript II (Invitrogen) according to the manufacturer's instructions. DNER primer sequences were: 5′-CTCCATTTCT GCATGGGTCT-3′ and 5′-GAGGAAACCTTGCCAAAACA-3′. MAG primer sequences were: 5′-AGCCCCTACCCCAAG AACTA-3′ and 5′GACGATATCCAGGACGCTGT-3′. HES1 primer sequences were 5′-AGCGGGCGCAGATGAC-3′ and 5′-CGTTCATGCACTCGCTGAA-3. Quantitative real-time polymerase chain reaction (PCR) was performed with an Applied Biosystems Prism 7900 HT Sequence Detection System using SYBR Green PCR Master Mix (Applied Biosystems, Foster City, CA, http://www.appliedbiosystems.com). The thermal cycling conditions were as follows: hold for 10 minutes at 95°C, followed by three-step PCR for 40 cycles of

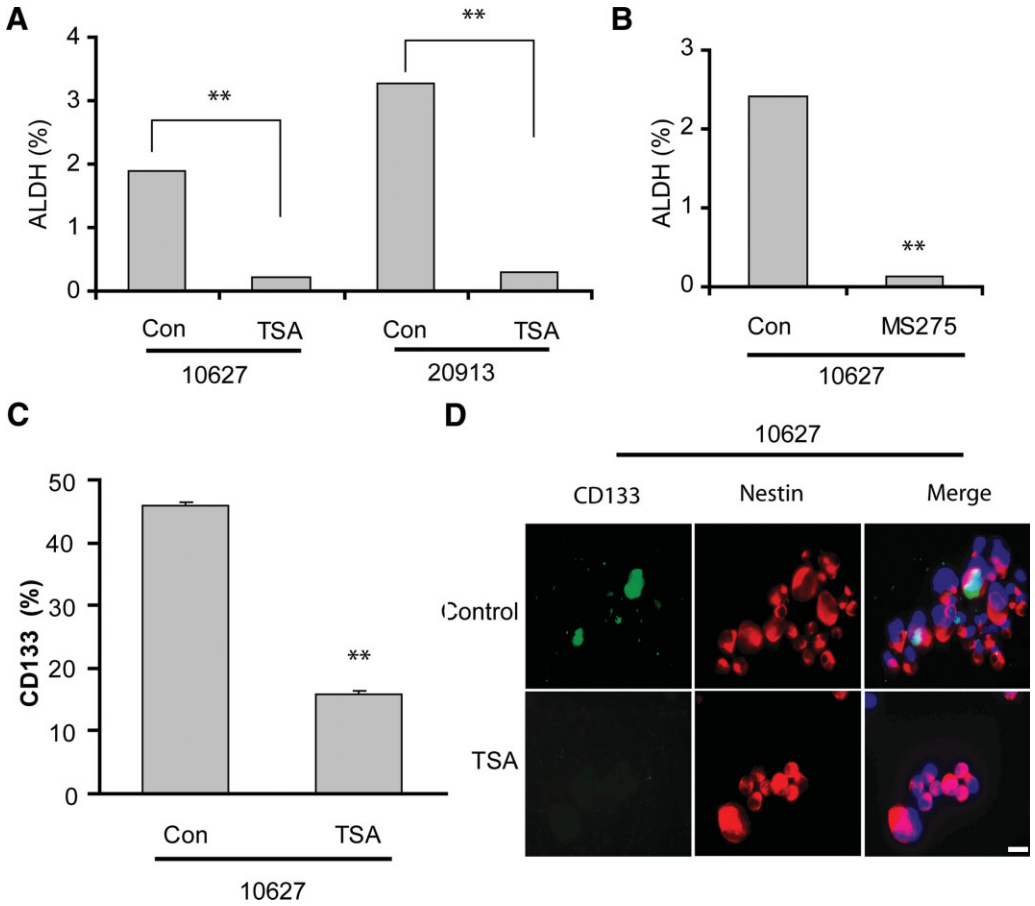

Figure 2. HDAC inhibition depletes GBM-derived neurospheres of cells expressing stem cell markers. GBM-derived neurosphere lines were passaged into neurosphere medium containing buffer only (Con) or either TSA (200 nM) or MS-275 (4 μM) and then cultured for an additional 3 days. Neurosphere cells were then dissociated and subjected to flow cytometry to detect ALDH-expressing cells **(A and B)** and CD133-expressing cells **(C)**. **(D):** Neurospheres were cultured in the presence of buffer only (control) or TSA as described above. Neurospheres that formed were collected by cytospin and subjected to immunofluorescence for CD133 and nestin. TSA depleted neurospheres of ALDH- and CD133-expressing cells. Bar = 20 μm. Data are shown as the mean $\pm$ standard error of the mean **(A–C)**. $^{**}p < .01$. Abbreviations: ALDH, aldehyde dehydrogenase; Con, control; GBM, glioblastoma; HDAC, histone deacetylase; TSA, trichostatin A.

95°C for 15 seconds, 55°C for 25 seconds, and 72°C for 30 seconds. Samples were amplified in triplicate and data were analyzed using the Applied Biosystems Prism Sequencer Detection Software Version 2.3 (Applied Biosystems). Human 18S rRNA was amplified as an endogenous control. Standard curves were prepared for each mRNA and 18S rRNA for each amplification to normalize relative gene expression to the 18S rRNA control.

Gene Expression Knockdown

Predesigned small interfering (si)RNA for human DNER was purchased from Ambion (ID 125934; Ambion, Austin, TX, http://www.ambion.com). The resulting double-stranded siRNA (50 nM) was transfected into cultured cells using siPort Lipid transfection agent (Ambion). Neurosphere cells were plated in duplicate in a six-well plate (10^5 cells per well) format for RNA analysis and in 48-well plates (1.5×10^4 cells per well) for growth assays. For each transfection, 32 μl siPort transfection reagent was mixed with 1.1 ml Optimum Medium (Gibco, Grand Island, NY, http://www.invitrogen.com) and incubated at room temperature for 20 minutes. Three microliters of 20 μM negative control siRNA (*Silencer* Negative Control #1 siRNA; Ambion) or DNER siRNA solution was added to the mixture, which was incubated at room temperature for another 20 minutes. The mixture was then added to cell medium and incubated for 48 hours prior to MTS assay or protein extraction. The silencing effect of the siRNA construct on DNER expression was confirmed by immunoblot analysis. The SiDNER sequence one (SiDNER.1) sense siRNA strand was 5′-GUGUGACCCCCUUCAGGCtt-3′ and the antisense siRNA strand was 3′-ttCACACUGGGG GGAAGUCCG-5′; the SiDNER.2 sense siRNA strand was 5′-GCAGUACGUGGGUACUUUCtt-3′ and antisense siRNA strand was 3′-ctCGUCAUGCACCCAUGAAAG-5′. The SiDeltex-1.1 sense siRNA strand was 5′-GGAUGUGGUUCGAAG AUACtt-3′ and the antisense siRNA strand was 3′-ctCCUAC ACCAAGCUUCUAUG-5′; the SiDeltex-1.2 sense siRNA strand was 5′-GCACCUUAAAAAGAGUAAGtt-3′ and the antisense siRNA strand was 3′-ttCGUGGAAUUUUUCUCA UUC-5′.

Tumor Xenografts

Female 4- to 6-week-old athymic nude mice were injected s.c. in the flank with 5×10^6 viable cells in 0.1 ml of phosphate-buffered saline (PBS). When tumors reached $\sim$50 mm^3, the mice were randomly divided into groups and treated with TSA (500 μg/kg in 0.2 ml PBS) or with solvent only as a control, i.p. daily as previously described [35]. Tumor sizes

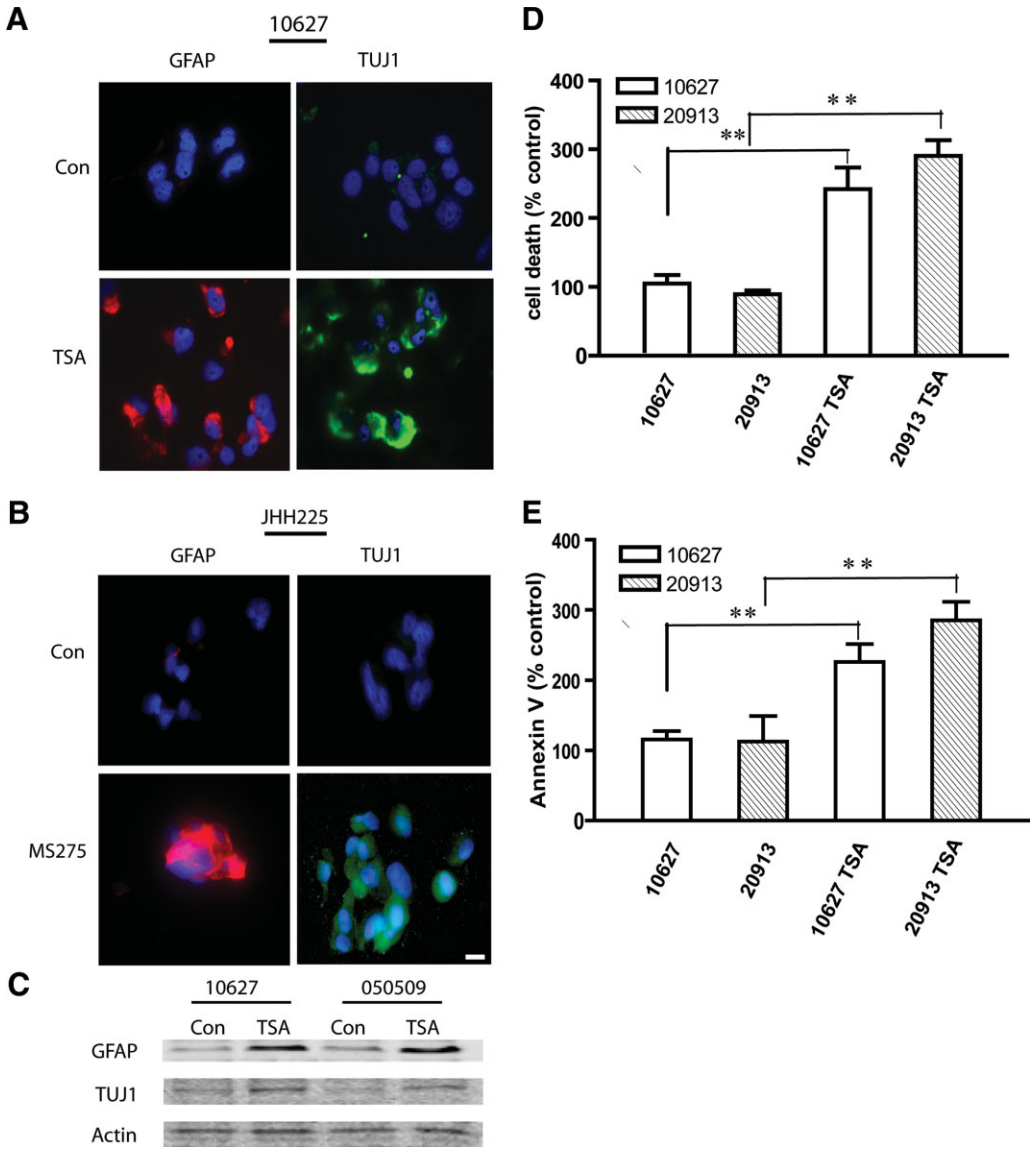

Figure 3. HDAC inhibitors induce GBM-derived neurosphere cell differentiation and apoptosis. Low passage primary neurospheres (JHH225) and neurosphere lines (050509 and 10627) were incubated with either TSA (200 nM) or MS-275 (4 μM) for 3 days. **(A, B):** Neurospheres and nonadherent cells were collected by cytospin and then stained with anti-GFAP (red) and anti-TuJ1 (green). Nuclei are stained blue. **(C):** Alternatively, whole cell proteins were isolated and subjected to immunoblot analysis using anti-GFAP or anti-TuJ1, and anti-actin. GFAP and TuJ1 expression are induced by HDAC inhibition. Bar = 20 μm. **(D):** Neurosphere cell viability was determined by trypan blue exclusion. **(E):** Neurosphere cell apoptosis was determined by Annexin V flow cytometry as described in Materials and Methods. TSA increased the fraction of trypan blue- and Annexin V-positive cells approximately two- to threefold. Data **(D, E)** are shown as the mean ± standard error of the mean. ** $p <$ .01. Abbreviations: Con, control; GBM, glioblastoma; GFAP, glial fibrillary acidic protein; HDAC, histone deacetylase; TSA, trichostatin A.

were determined weekly by measuring two dimensions—length (a) and width (b)—and volume (V) was estimated using the formula $V = ab^2/2$ [36]. At the end of each experiment, tumors were excised and weighed.

For intracranial xenografts, SCID/NCR immunodeficient mice received 5,000 viable neurosphere cells in 5 μl of culture medium by stereotactic injection to the right caudate/putamen. In certain experiments, cells were treated with TSA (200 nM) for 3 days or transfected with *DNER* expression plasmid 48 hours prior to implantation. Cell viability was determined by trypan blue dye exclusion. Groups of mice (n = 10) were sacrificed at the indicated times and the brains were removed for histologic studies. Tumor sizes were quantified by measuring tumor cross-sectional areas on hematoxylin and eosin-stained cryostat sections from perfusion-fixed brains using computer-assisted image analysis as previously described [36]. Volumes were estimated based on the formula: volume = (square root of maximum cross-sectional area)^3 as previously described [36]. All animal protocols used in this study were approved by the Johns Hopkins School of Medicine Animal Care and Use Committee.

Immunofluorescence and Immunohistochemistry

The expression and cellular localization of CD133 (Santa Cruz Biotechnology), GFAP, and TuJ1 were determined by immunofluorescence. Neurosphere cells were plated on coverslips or collected by cytospin onto glass slides. The cells were fixed with 4% paraformaldehyde for 10 minutes

and permeabilized with PBS containing 7.5% glycine and 0.5% Triton X-100 for 30 minutes. The cells were then incubated with primary antibody in staining solution (1% bovine serum albumin [BSA] with 0.1% NP-40) for 2 hours and then incubated with appropriate corresponding secondary antibodies (fluorescein isothiocyanate [FITC]-conjugated goat anti-mouse and Texas Red-conjugated goat anti-rabbit) for 30 minutes. Coverslips were placed with Vectashield Antifade solution containing 4′,6-diamidino-2-phenylindole (Vector Laboratories, Burlingame, CA, http://www.vectorlabs.com).

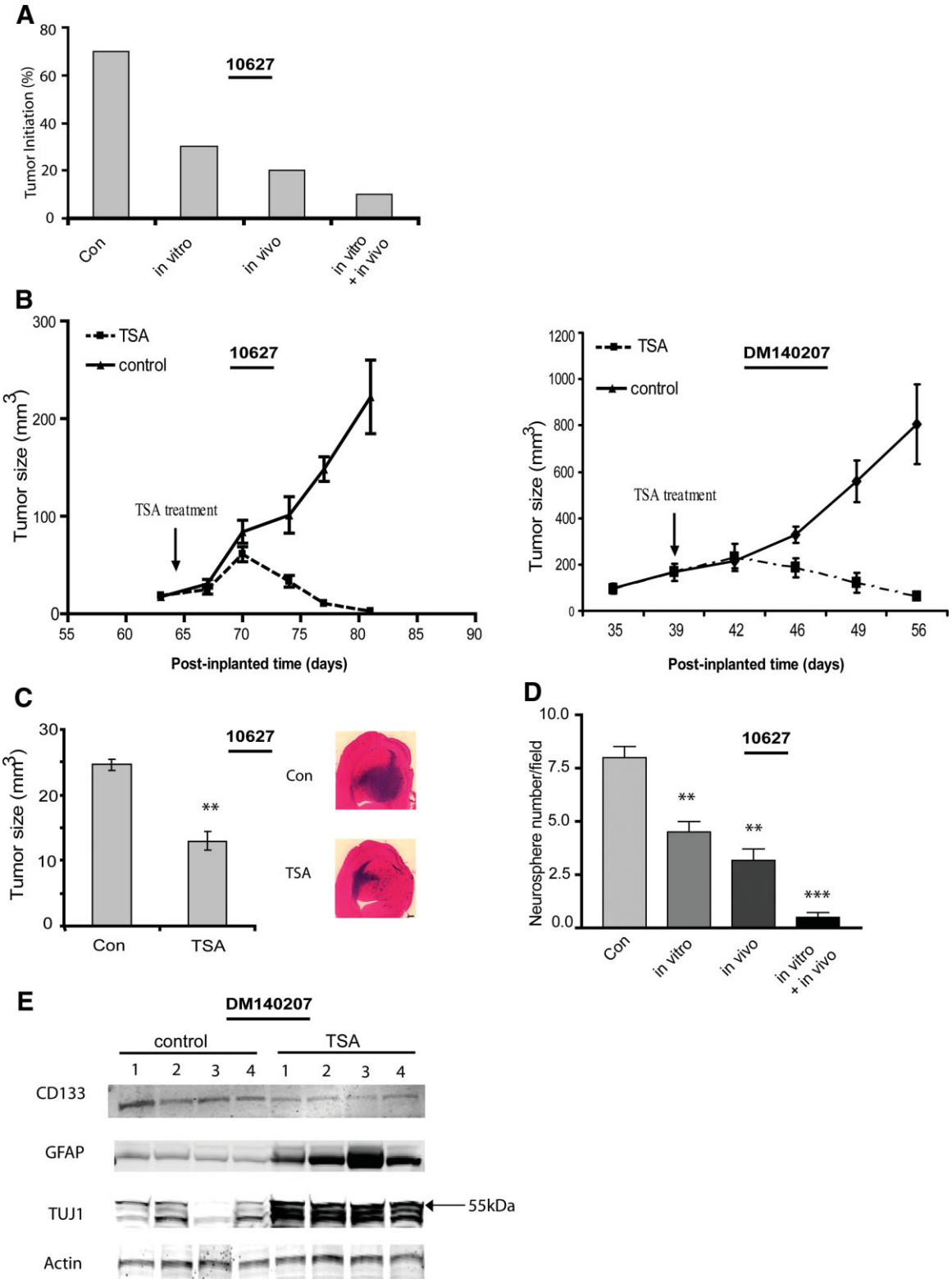

Figure 4.

Immunofluorescence was detected by fluorescent microscopy using Axiovision software (Carl Zeiss, Jena, Germany, http://www.zeiss.com).

Flow Cytometry

Flow cytometry was performed to determine the percentage of cells expressing ALDH using the Aldefluor reagent according to the manufacturer's specifications (Stem Cell Technologies, Vancouver, BC, Canada, http://www.stemcell.com). Aldefluor substrate (0.625 g/ml) was added to neurosphere cells suspended in Aldefluor assay buffer (10^6 cells/ml). Cells were then incubated for 20-30 minutes at 37°C to allow the conversion of Aldefluor substrate to its intracellular fluorescent product [37]. Cell fluorescence was measured using an LSR flow cytometer equipped with 424/44 nm band pass and 670 nm long pass optical filters (Omega Optical, Brattleboro, VT, http://www.omegafilters.com). ALDH values are presented as mean fluorescence intensity.

Flow cytometry analysis of CD133 expression was performed with phycoerythrin-conjugated anti-CD133 antibody (clone 293C3; Miltenyi Biotec, Auburn, CA, http://www.miltenyibiotec.com) following the manufacturer's protocol. Briefly, up to 5×10^6 dissociated neurosphere cells were suspended in 100 μl assay buffer (PBS, pH 7.2, 0.5% BSA, 2 mM EDTA) and 10 μl of the CD133 antibody were added. The cells were gently rotated for 10 minutes in the dark at 4°C, washed by adding 1 ml of assay buffer, and then pelleted at 300g for 10 minutes. The cell pellet was resuspended in PBS and analyzed by a FACSCalibur fluorescence-activated cell sorting (FACS) flow cytometer (BD Biosciences, San Jose, CA, http://www.bdbiosciences.com). Data were quantified using CellQuest software (BD Biosciences).

Cell death was quantified using the annexin V-FITC/propidium iodide (PI) apoptosis kit (BD Bioscieneces, San Diego, http://www.bdbiosciences.com) according to the manufacturer's instructions. Briefly, dissociated cells were resuspended in annexin V binding buffer (150 mM NaCl, 18 mM $CaCl_2$, 10 mM HEPES, 5 mM KCl, 1 mM $MgCl_2$). FITC-conjugated annexin V (1 μg/ml) and PI (50 μg/ml) were added to cells, which were incubated for 30 minutes at room temperature in the dark and subjected to FACScan analysis to quantify the annexin V-positive/PI^-negative cells.

Statistical Analysis

Data were analyzed using parametric statistics with one-way analysis of variance. Post hoc tests included Student's *t*-test and the Tukey multiple comparison tests as appropriate using Prizm (GraphPad Software Inc., San Diego, CA, http://www.graphpad.com). All experiments reported here represent at least three independent replications. All data are represented as the mean value ± standard error of mean. Significance was set at $p < .05$.

Results

HDAC Inhibition Inhibits GBM-Derived Neurosphere Formation

Histone modification influences the phenotype of normal stem and progenitor cells and may play substantial roles in the initiation, growth, and malignant progression of cancer. We examined the effect of histone deacetylase inhibition on the growth of GBM-derived neurosphere cells under neurosphere growth conditions. TSA and MS-275 each inhibited neurosphere cell growth in a concentration- and time-dependent manner. When neurosphere cells were treated for 72 hours, the 50% inhibitory concentration (IC_{50}) values for TSA and MS-275 were ~200 nM and ~3.5 μM, respectively, as determined by MTS assay (supporting information Fig. 1A). Exposing neurosphere cultures to either drug at its approximate IC_{50} for 144 hours inhibited neurosphere cell growth by 82%–86% ($p < .001$) (Fig. 1A).

TSA and MS-275 potently inhibited GBM neurosphere cell growth in immobilized colony formation assays (Fig. 1B). Treating cultures with TSA (200 nM) continuously for 14 days inhibited the formation of colonies (≥100 μm diameter) by 95%–98%. Pretreating cells with TSA for 3 days immediately prior to initiating the assay inhibited colony formation by 88%–90%. Both TSA and MS-275 increased GBM neurosphere cell histone acetylation three- to fivefold under these experimental conditions, consistent with their HDAC inhibitory actions (supporting information Fig. 1B).

HDAC Inhibition Induces GBM-Derived Neurosphere Cell Differentiation and Depletes Neurospheres of Stem-Like Cells

Possible mechanisms by which HDACIs reduce GBM-derived neurosphere cell growth and neurosphere formation include the inhibition of neurosphere proliferation, the induction of neurosphere cell death, the induction of neurosphere cell differentiation, and the depletion of the stem-like cell pool in heterogeneous neurosphere cultures. We examined the effects

Figure 4. HDAC inhibitors reduce tumor propagation by GBM-derived neurospheres and deplete tumor xenografts of neurosphere-forming stem-like cells. **(A):** GBM-derived neurospheres were treated with or without TSA (200 nM) for 4 days in vitro. Equal numbers of viable cells (5×10^6) were implanted s.c. to Nu/nu mice ($n = 10$) and animals began treatment with or without TSA (0.5 mg/kg per day i.p.) 5 days after cell implantation. The percentage of tumors formed over 8 weeks was quantified. Seventy percent of controls (buffer-treated only) formed tumors. Transient exposure to TSA before cell implantation (in vitro) reduced tumor propagation to 30%. Tumor propagation was further inhibited by in vivo TSA. **(B):** When mice bearing pre-established s.c. xenografts (~50 mm^3) were treated with TSA (0.5 mg/kg per day i.p.) the tumors ($n = 6$) regressed within 10 days of treatment initiation. **(C):** GBM-derived neurospheres were treated for 4 days with or without TSA (200 nM) in vitro. Viable neurosphere cells (5×10^3) were then implanted to the caudate/putamen. After 6 weeks, the mice were sacrificed. Histological analysis revealed that tumor propagation rates by control- and TSA-treated neurosphere cells were 80% and 50%, respectively. Tumors propagated by TSA-treated neurospheres were significantly smaller than tumors derived from control neurospheres ($p < .01$). **(D):** s.c. xenografts were established from GBM-derived neurospheres as in **(A)**. After 8 weeks in vivo, xenografts were dissected and equal numbers of dissociated cells were used to establish primary cultures in neurosphere growth medium. Neurospheres formed after one passage were immobilized in agar and those measuring >100 μm diameter were quantified by computer-assisted morphometry as described in Figure 1. All TSA treatment conditions depleted the tumor xenografts of neurosphere-forming stem-like cells. **(E):** Nu/nu mice bearing GBM xenografts derived from neurosphere cells were treated with TSA as described in **(B)**. After 19 days of treatment, residual tumors were resected and whole tumor protein extracts were assayed for GFAP, TuJ1, CD133, and actin by immunoblot analysis. TSA therapy in vivo decreased tumor expression of CD133 and increased tumor expression of differentiation markers. Note that, in whole tumor protein extracts, anti-TuJ1 identified approximately three species at and below 55 kDa. Data are shown as the mean ± standard error of the mean. **(B–D)**. $^{**}p < .01$ and $^{***}p < .001$, compared with controls. Abbreviations: Con, control; GBM, glioblastoma; GFAP, glial fibrillary acidic protein; HDAC, histone deacetylase; TSA, trichostatin A.

of HDAC inhibition on GBM neurosphere cell expression of markers associated with the neoplastic stem-like cell phenotype [9, 38]. Under control neurosphere growth conditions, ALDH was expressed by ~2%–3% of neurosphere cells, as determined by quantitative Aldefluor flow cytometry assay. The percentage of ALDH-expressing cells diminished approximately tenfold to ~0.2%–0.4% when cultured for 72 hours with either TSA or MS-275 (Fig. 2A, 2B). CD133 has been linked to stem-like, tumor-initiating GBM cells, and nestin is an intermediate filament protein expressed by both neurosphere stem and progenitor cells. We therefore also examined the effects of HDAC inhibition on CD133 and nestin. Flow cytometry analysis showed that CD133 was expressed by ~45% of neurosphere cells under control neurosphere growth conditions, and the percentage of $CD133^+$ cells dropped approximately threefold to ~15% when cultured for 72 hours with TSA (Fig. 2C). The depletion of $CD133^+$ cells was confirmed by immunofluorescence (Fig. 2D). In contrast, the number of nestin-expressing cells was relatively preserved following treatment with TSA (Fig. 2D).

We also examined the effects of TSA and MS-275 on neurosphere cell expression of the astrocyte marker GFAP and the neuronal marker β-tubulin III (TuJ1). Expression levels of both differentiation markers were substantially increased 72 hours after adding either HDACI to standard neurosphere culture medium, as detected by immunofluorescence (Fig. 3A, 3B). Immunoblot analyses confirmed that GFAP and TuJ1 protein expression increased in response to HDAC inhibition (Fig. 3C).

HDAC inhibition also affected the viability of neurosphere cells and induced neurosphere cell apoptosis. TSA (200 nM, 72 hours) increased the fraction of injured and apoptotic cells two- to threefold, as evidenced by trypan blue staining and annexin V flow cytometry, respectively (Fig. 3D, 3E).

HDAC Inhibition Abrogates the Tumor-Forming Capacity of GBM-Derived Neurospheres

A defining phenotype of neoplastic stem-like cells is their ability to propagate and maintain malignant tumors in vivo. We and others have shown that GBM-derived neurospheres, including the neurospheres used in this current study, form tumor xenografts that recapitulate many features of human GBM (e.g., high degree of invasiveness, necrosis) [17, 29, 39]. We examined the effect of TSA on the tumorigenicity of GBM-derived neurosphere cells in immune-deficient mice. s.c. xenografts were used in these initial experiments to allow us to both assess tumor formation/growth in real time and culture primary neurospheres from resected xenografts. Animals received equal numbers of viable (trypan blue-negative) control- or TSA-treated neurosphere cells (4×10^6 cells per implantation site). The effect of in vivo TSA treatment was also examined. Results are shown in Figure 4A. Control neurospheres formed measurable tumors in 70% of animals. Pretreating neurospheres with TSA (200 nM) for 4 days prior to cell implantation reduced tumorigenicity to 30%. Implanting control neurosphere cells and then treating animals with TSA (0.5 mg/kg per day i.p.) beginning on postimplantation day 3 reduced tumorigenicity to 20%. Combining in vitro and in vivo TSA therapy generated measurable tumors in only 10% of animals. Furthermore, when mice bearing pre-established neurosphere-derived xenografts (9 weeks postimplantation) were treated with TSA (0.5 mg/kg per day i.p.), tumors regressed within 10 days of treatment initiation (Fig. 4B). We asked if TSA similarly affects the growth of neurosphere-derived orthotopic tumor xenografts. Treating GBM-derived neurosphere cultures with TSA (200 nM) for 4 days prior to cell implantation reduced tumorigenicity from 80% to 50%. On postimplantation day 60, tumors that formed from TSA-treated cells were ~50% smaller than control tumors (Fig. 4C).

The reduction in tumor initiation and tumor growth rates suggested that xenografts derived from TSA-treated cells might be relatively depleted of their tumor-propagating stem-like cells. TSA treatment significantly depleted tumor xenografts of cells with the capacity to generate large neurospheres (>100 μm diameter) (Fig. 4D), and the magnitude of depletion mirrored the effect of TSA on tumor initiation rates (compare Fig. 4A with Fig. 4D). The effects of TSA on tumor xenograft cell expression of CD133 and the differentiation markers GFAP and TuJ1 were assessed by immunoblot analysis of xenograft protein extracts. Both GFAP and TuJ1 expression increased four- to sevenfold and CD133 expression decreased approximately two- to threefold in response to TSA treatment (Fig. 4E). These in vivo effects parallel the effects of HDAC inhibition on neurosphere cells observed in vitro.

DNER Signaling Is Induced by HDAC Inhibition and Regulates GBM-Derived Neurosphere Cell Growth and Differentiation

The effects of HDAC inhibition on GBM-derived neurosphere formation, differentiation, and tumor propagation led us to use HDACIs to identify gene expression patterns that regulate the tumor-initiating phenotype of GBM-derived neurospheres. We examined the effect of TSA on the gene expression profiles of two GBM-derived neurosphere lines using Affymetrix gene expression arrays. The expression levels of 36 genes were found to be changed threefold of greater by TSA in both neurosphere lines. One of these genes, *DNER*, was induced five- to eightfold, as determined by quantitative RT-PCR (supporting information Fig. 2A). Noncanonical Notch pathway activation by DNER is mediated, in part, by the transcription factor Deltex. Immunoblot and immunofluorescence analyses showed that both DNER and Deltex-1 were induced by TSA treatment in established GBM-derived neurosphere lines and in low passage neurospheres derived from a human malignant glioma (Fig. 5A–5C). Deltex-1 and DNER were similarly induced by MS-275. We found that both TSA and DNER directly activated noncanonical Notch signaling in GBM-derived neurosphere cell lines, as evidenced by Deltex-dependent induction of the myelin-related protein MAG [40, 41]. MAG expression increased ~15-fold in response to TSA and ~13-fold following transfection with DNER (Fig. 5D, 5E). Neither TSA nor DNER transfection induced expression of the canonical Mastermind-dependent, Deltex-independent Notch pathway target Hes1 (supporting information Fig. 3A, 3B) [42]. siRNA-mediated Deltex expression knockdown (supporting information Fig. 2D) inhibited MAG induction by both TSA and DNER (Fig. 5D, 5E, using SiDeltex-1.1; supporting information Fig. 3C, 3D, using another siRNA, SiDeltex-1.2). Taken together, these findings indicate that HDAC inhibition activates a noncanonical DNER/Deltex signaling pathway in GBM-derived neurospheres.

We used a gene expression knockdown approach to determine if DNER mediates the GBM neurosphere response to HDAC inhibition. Transient transfection of GBM neurospheres with anti-DNER siRNA (SiDNER) potently inhibited the low level of basal DNER expression and also inhibited DNER induction in response to TSA (supporting information Fig. 2B, 2C). We asked if SiDNER altered neurosphere growth inhibition following HDAC inhibition. GBM neurosphere

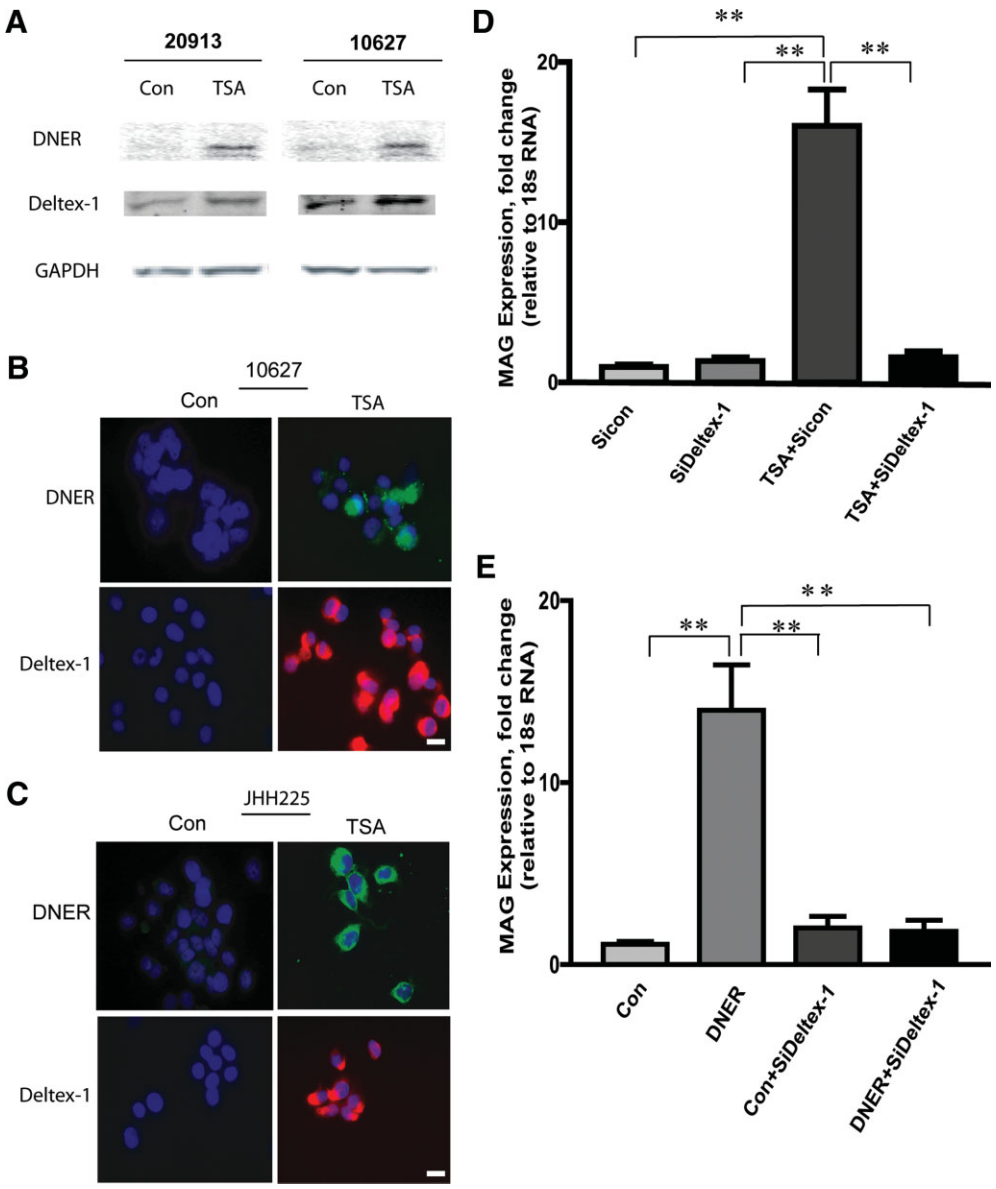

Figure 5. HDAC inhibition induces DNER and Deltex-1 protein expression in GBM-derived neurospheres. Low passage primary neurospheres (JHH225) and neurosphere lines (20913 and 10627) were treated with or without TSA (200 nM) for 4 days. **(A):** Equal amounts of total cell protein were assayed for DNER, Deltex-1, and GAPDH by immunoblot analysis. **(B, C):** Control- and TSA-treated neurospheres were collected by cytospin and subjected to anti-DNER (green) and anti-Deltex-1 (red) immunofluorescence. Nuclei are stained blue. Bar = 20 μm. **(D):** GBM-derived neurosphere cells (10627) were incubated with or without TSA for 72 hours. Eight hours after adding TSA, cells were treated with or without SiDeltex-1.1 (30 nM) for a total of 64 hours. MAG mRNA was then quantified by real-time reverse transcription-polymerase chain reaction. TSA induced MAG expression ~15-fold and SiDeltex-1 inhibited MAG induction. **(E):** GBM-derived neurosphere cells were transfected with full-length DNER cDNA with or without SiDeltex-1.1. Seventy-two hours later, MAG mRNA levels were determined as described in **(D)**. MAG expression increased ~13-fold in response to DNER. SiDeltex-1 inhibited MAG induction by DNER. $^{**}p < .01$. Similar responses to Deltex-1 expression knockdown were obtained using a second Deltex-targeting sequence, SiDeltex-1.2 (see supporting information Fig. 4D, 4E). Abbreviations: Con, control; DNER, Delta/Notch-like epidermal growth factor-related receptor; GAPDH, glyceraldehyde-3-phosphate dehydrogenase; GBM, glioblastoma; HDAC, histone deacetylase; TSA, trichostatin A.

cells were treated with TSA (200 nM, 72 hours) with or without SiDNER (50 nM, 48 hours). The cells were then transferred to standard neurosphere growth medium for 7 days. Results are shown in Figure 6A. Neurosphere formation was inhibited by TSA and not affected by SiDNER alone. However, cells treated with both TSA and SiDNER formed threefold more neurospheres than cells treated with TSA and control siRNA. Thus, preventing DNER induction with SiDNER partially blocked the growth inhibitory effects of TSA.

DNER was found to induce the differentiation of GBM neurosphere cells as assessed by GFAP and TuJ1 expression (Fig. 6B, 6D). GFAP and TuJ1 expression levels increased approximately threefold and approximately fourfold, respectively, as determined by immunoblot analysis. Forced expression of DNER in neurosphere cells reduced their proportion of $CD133^+$ cells by ~50% (Fig. 6C). Mirroring the ability of SiDNER to reverse the inhibitory effect of TSA on neurosphere cell colony formation, SiDNER was also found to

reverse TSA-induced neurosphere cell differentiation, as determined by GFAP and TuJ1 immunofluorescence (Fig. 6D, using SiDNER.1, and supporting information Fig. 4, using another siRNA, SiDNER.2). Conversely, transfecting neurosphere cells with DNER cDNA induced GFAP and TuJ1 expression, mimicking the response to TSA treatment (Fig. 6D). In contrast to its effects on neurosphere cell differentiation, DNER had no detectable effect on neurosphere cell viability or apoptosis. SiDNER did not alter the viability of control- or TSA-treated neurosphere cells (Fig. 6E). Forced

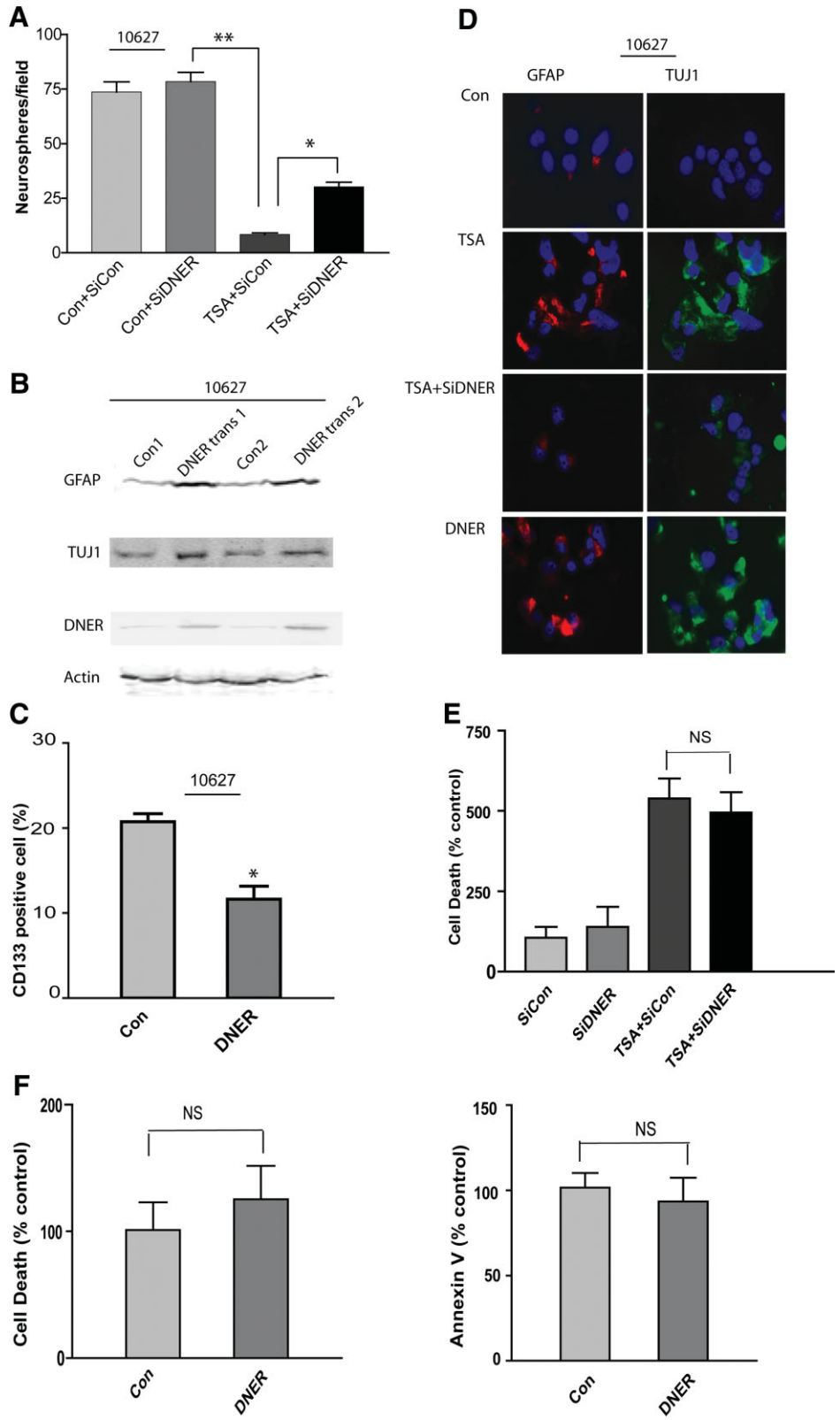

Figure 6.

DNER expression did not alter the viability or annexin V staining of neurosphere cells (Fig. 6F). Together, these loss- and gain-of function results strongly suggest that DNER signaling pathways modulate GBM stem-like cell growth, differentiation, and possibly tumor propagation and maintenance.

Finally, we examined the effect of DNER upregulation on the growth of orthotopic tumor xenografts derived from GBM neurospheres. Mice received equal numbers of viable GBM neurosphere cells by stereotaxic injection to the caudate/putamen 72 hours after the cells were transfected with control or full-length *DNER* plasmid expression vectors. Tumor volumes assessed on postimplantation day 68 showed that tumor xenografts derived from DNER-transfected cells were ~60% smaller than controls (Fig. 7).

Discussion

Glioblastoma multiforme is the most common and aggressive of the primary brain cancers. Despite dramatic reductions in tumor burden with surgery, radiotherapy, and chemotherapy, tumor recurrence is almost universal [43]. The high frequency of GBM recurrence reflects the inherent chemo-/radiation resistance of at least a subset of the invasive cancer cells that inevitably remain after aggressive surgery. According to the cancer stem-cell hypothesis, only a small number or, at its extreme interpretation, a single remaining tumor cell with stem-like properties can ultimately result in the recurrence of a heterogeneous GBM. There has been considerable progress in identifying the biological and molecular features of GBM cell subpopulations with stem-like properties since they were isolated using neurosphere growth conditions and shown to efficiently propagate tumor xenografts contemporaneously in 2004 by Singh et al. [3] and Galli et al. [10]. Perhaps the most clinically relevant features of GBM-derived stem-like cells identified to date are their ability to efficiently form tumor xenografts with the complex histologic features of human GBM and their inherent resistance to chemotherapy and radiation therapy. The resistance of neoplastic stem-like cells to DNA-damaging agents has been attributed in part to Chk1/2-dependent DNA repair mechanisms in GBM-derived cells [14] and to Wnt/β-catenin signaling in breast cancer-derived cells [44]. Neurodevelopmental pathways regulate GBM-derived stem-like cells. Among these are the Hh and canonical Notch/Mastermind pathways, found to maintain the cancer stem-cell phenotype, and bone morphogenetic proteins, which induce their differentiation and inhibit their tumor-initiating potential [17, 29, 39, 45]. Effort is under way to translate these discoveries to reduce the tumor-initiating potential of the stem-like cell subpopulation through either differentiation and/or chemo-/radiation sensitization in conjunction with conventional treatments.

We now show that histone deacetylase inhibition induces GBM-derived stem-like cells to differentiate, undergo apoptosis, and loose their capacity to both grow as neurospheres and initiate tumor xenografts. These cell responses mimic, to some degree, the responses of normal neural stem/progenitor cells to HDAC inhibition [20, 26, 46], supporting the current concepts regarding shared regulatory mechanisms and possibly overlapping origins between normal neural and GBM-derived neoplastic stem cells. Our results are interesting in the context of the recent findings of Lee et al. [17], showing that epigenetic gene regulation via promoter methylation can alter the differentiation and tumor-initiating capacity of GBM stem-like cells. The HDACIs used in our experiments, MS-275 (now available as Sndx-275; Syndax Pharmaceuticals, Waltham, MAhttp://www.syndax.com) and TSA, also have antitumor activity against tumor xenograft models derived from cancer cells maintained under traditional serum-containing culture conditions [47, 48]. HDAC inhibition can broadly induce tumor suppressors and inhibit tumor promoters regardless of cell stemness. It is also possible that the antitumor effects of HDACIs in traditional xenograft models reflect, at least in part, the targeting of tumor-initiating cell subpopulations with stem-like characteristics within traditional cancer cell lines [49, 50]. HDACIs, including Sndx-275 and suberoylanilide hydroxamic acid, are currently in clinical trials for solid malignancies. Our findings expand the influences of HDACIs to GBM stem-like cells and the nonclassical Notch ligand DNER. The ability of HDACIs to cross the blood–brain barrier makes them applicable to clinical testing in brain tumor patients [51].

Our conclusions that HDAC inhibition and DNER, an HDACI-induced gene product, differentiate GBM stem-like cells and inhibit their tumor-initiating phenotype are based on complementary biological and molecular endpoints. In contrast to hematopoietic neoplastic stem cells, cell surface markers that reliably identify tumor-initiating stem cells in solid cancers are lacking. Therefore, our approach emphasized experimental endpoints that are well accepted to consistently associate with the neoplastic stem-like phenotype, namely, the formation of large neurospheres in vitro and tumor xenograft initiation by neurosphere-derived cells. CD133 and ALDH, markers that correlate with neoplastic neurosphere growth and

Figure 6. DNER regulates GBM-derived neurosphere cell growth and differentiation and not apoptosis. **(A):** Neurospheres (line 10627) were dissociated, transfected with control siRNA (SiCon) or with anti-DNER siRNA (SiDNER), and replated in neurosphere growth medium with or without TSA (200 nM) as shown. Seven days later, neurospheres were immobilized in soft agar and those measuring >100 μm diameter per low powered field were quantified by computer-assisted morphometry. Cultures treated with TSA plus SiDNER contained threefold more large neurospheres than cultures treated with TSA alone. DNER expression inhibition rescues neurosphere cells from the growth-inhibiting effects of TSA. **(B):** Neurosphere cells were transfected with control plasmid or with plasmid containing full-length DNER cDNA. Sixty hours later, total cell lysates were assayed for GFAP, TuJ1, and actin by immunoblot analysis. Transgenic DNER induces both GFAP and TuJ1 expression. **(C):** Neurosphere cells were transfected with control plasmid or with DNER as in **(B)**. Forty-eight hours later, neurospheres and nonadherent cells were collected, dissociated, and subjected to flow cytometry for CD133. DNER expression reduces the fraction of $CD133^+$ cells. **(D):** Neurosphere cells were transfected with TSA with or without SiDNER or transfected with full-length DNER cDNA and then grown under neurosphere growth conditions for 7 days. Nonadherent cells and neurospheres were then collected by cytospin and stained for the differentiation markers GFAP and TuJ1. DNER expression inhibition reversed TSA-induced differentiation and expressing full-length DNER induced differentiation. **(E):** GBM-derived neurospheres (line 10627) were dissociated, transfected with control siRNA (SiCon) or with anti-DNER siRNA (SiDNER), and replated in neurosphere growth medium with or without TSA (200 nM) as shown. Sixty hours later, neurosphere cell viability was determined by trypan blue exclusion. SiDNER did not alter the fraction of trypan blue-positive cells in either control- or TSA-treated neurospheres. **(F):** Neurosphere cells were transfected with control plasmid or with plasmid containing full-length DNER cDNA. Sixty hours later, cell viability was determined by trypan blue staining and apoptosis was determined by annexin V flow cytometry. Forced DNER expression had no effect on either parameter of cell viability. Data are shown as the mean ± standard error of the mean **(A, C)**. Bar, 20 μm; $*p < .05$; $**p < .01$; NS, $p > .05$. Abbreviations: Con, control; DNER, Delta/Notch-like epidermal growth factor-related receptor; GAPDH, glyceraldehyde-3-phosphate dehydrogenase; GBM, glioblastoma; GFAP, glial fibrillary acidic protein; siRNA, small interfering RNA; TSA, trichostatin A.

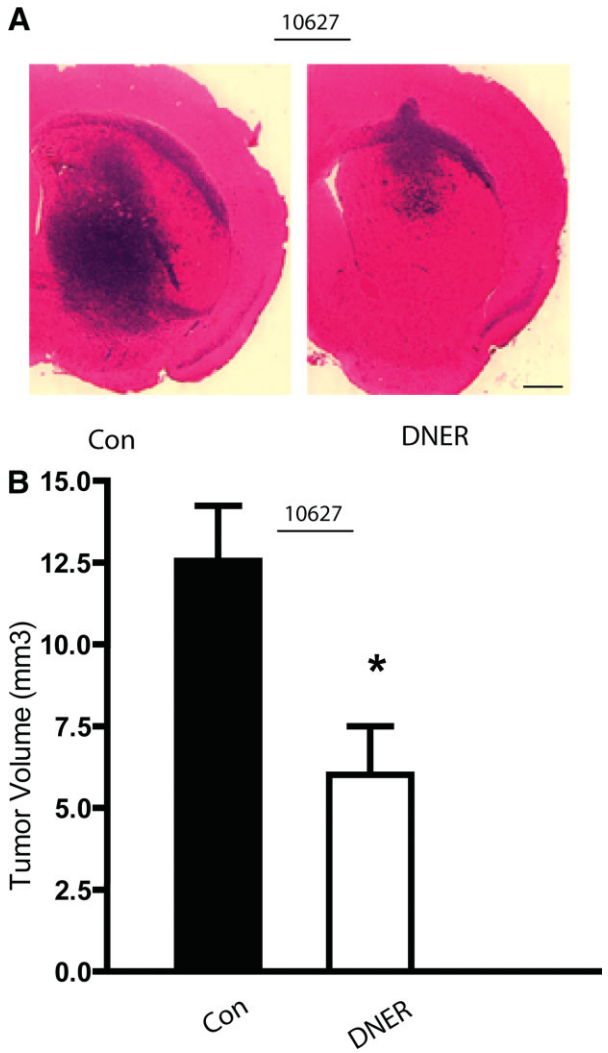

Figure 7. Transgenic DNER inhibits the growth of orthotropic tumor xenografts derived from GBM neurospheres. GBM-derived neurosphere cells (10627) were transfected with full-length DNER cDNA (or control plasmid). Twenty-four hours later, cells were dissociated and implanted to the right striatum of SCID/beige mice (5×10^3 viable cells/animal). **(A):** Animals were sacrificed 64 days later and tumors were identified in brain sections stained with hematoxylin & eosin. Bar = 100 μm. **(B):** Tumors derived from DNER-transfected cells were significantly smaller than controls. Data are shown as the mean ± standard error of the mean. *$p < .05$. Abbreviations: Con, control; DNER, Delta/Notch-like epidermal growth factor-related receptor; GBM, glioblastoma.

tumor initiation, were also examined and found to be consistently lost, whereas the neuronal and glial differentiation markers TuJ1 and GFAP were consistently induced in response to HDAC inhibition and DNER expression. That similar results were obtained using (a) multiple human GBM-derived neurosphere lines and low passage neurosphere cultures established at different institutions, (b) in vitro and in vivo model systems, (c) two chemically distinct HDACIs, and (d) both DNER gain and loss of function renders confidence in their broad applicability to cellular models in vitro and more biologically complex tumors in vivo.

The effects of HDAC inhibition can be broad and not limited to proliferation inhibition and differentiation. Consistent with this is our finding that HDAC inhibition also induced GBM neurosphere cell death via a predominantly apoptotic mechanism. In contrast to its effects on cell differentiation, the HDAC-induced gene product DNER had no apparent effects of neurosphere cell viability. We are currently exploring in more detail the transcriptional events downstream of HDAC inhibition specifically responsible for GBM neurosphere cell death. Understanding the molecular determinants that control whether GBM neurosphere cells die or differentiate will likely translate to more effective strategies for targeting neoplastic stem-like cells.

We used the effects of HDAC inhibition on gene expression to identify specific gene products that potentially regulate the GBM stem-like cell phenotype. We show, for the first time, that DNER functions as a tumor suppressor and differentiating factor in GBM-derived neurosphere cells. DNER is a single-pass transmembrane Notch ligand containing 10 extracellular EGF-like repeats and lacking the Delta, Serrate, Lag-2 (DSL) Notch-binding motif that characterizes classical Notch ligands [52]. DNER is strongly expressed by cerebellar Purkinje cells and regulates cerebellar development and neurodevelopmental interactions between Purkinje cells and Bergmann glia that express Notch. Notch ligands induce Notch receptor cleavage by metalloprotease and γ-secretase releasing the Notch intracellular domain (NICD) that transduces to canonical (CSL/NICD/Mastermind transcriptional complex) and noncanonical (NF-κB/NICD and CSL/NICD/Deltex transcriptional complex) pathways. Signaling through the classical Notch pathway has multiple contextual functions, such as stem cell self-renewal, progenitor cell fate determination, and terminal differentiation of proliferating cells [53–55]. DNER promotes Bergmann glial process formation in vitro via a Deltex-dependent mechanism. Our findings that Deltex-1 is induced along with DNER by HDAC inhibition and that DNER induces expression of the Deltex target gene *MAG* support a role for a noncanonical signaling mechanism.

A complex role for Notch signaling in central nervous system malignancies is emerging. High-grade gliomas express the DSL-containing Notch ligand Jagged, Notch receptors, and downstream target genes induced by CSL/NICD/Mastermind in patterns that have been found to correlate with malignant grade and poor prognosis [56, 57]. Fan et al. [45] found that inhibiting canonical Notch signaling with γ-secretase inhibitors can deplete embryonal brain tumor cell lines of their neoplastic stem-like cells and tumor-initiating capacity. These findings support an oncogenic role for classical Notch signaling in certain brain tumor subtypes and contrast the tumor suppressive effects of DNER reported here in GBM-derived neurospheres. Developing a detailed framework for the oncogenic and tumor-suppressing effects of canonical and noncanonical Notch signaling in brain cancer stem-like cells will require a more complete understanding of the cell type- and context-dependent actions and interactions of the numerous Notch ligands, Notch receptors, and their downstream effectors.

Acknowledgments

This work was funded by NIH grants NS43987 (J.L.) and NS055089 (C.G.E.), The Maryland Stem Cell Research Fund (J.L.), and The Brain Tumor Funders Collaborative.

Disclosure of Potential Conflicts of Interest

The authors indicate no potential conflicts of interest.

References

1 Marx J. Cancer research. Mutant stem cells may seed cancer. Science 2003;301:1308–1310.
2 Lapidot T, Sirard C, Vormoor J et al. A cell initiating human acute myeloid leukaemia after transplantation into SCID mice. Nature 1994; 367:645–648.
3 Singh SK, Clarke ID, Hide T et al. Cancer stem cells in nervous system tumors. Oncogene 2004;23:7267–7273.
4 Reya T, Morrison SJ, Clarke MF et al. Stem cells, cancer, and cancer stem cells. Nature 2001;414:105–111.
5 Bonnet D, Dick JE. Human acute myeloid leukemia is organized as a hierarchy that originates from a primitive hematopoietic cell. Nat Med 1997;3:730–737.
6 Park CH, Bergsagel DE, McCulloch EA. Mouse myeloma tumor stem cells: A primary cell culture assay. J Natl Cancer Inst 1971;46: 411–422.
7 Al-Hajj M, Wicha MS, Benito-Hernandez A et al. Prospective identification of tumorigenic breast cancer cells. Proc Natl Acad Sci USA 2003;100:3983–3988.
8 Ignatova TN, Kukekov VG, Laywell ED et al. Human cortical glial tumors contain neural stem-like cells expressing astroglial and neuronal markers in vitro. Glia 2002;39:193–206.
9 Hemmati HD, Nakano I, Lazareff JA et al. Cancerous stem cells can arise from pediatric brain tumors. Proc Natl Acad Sci USA 2003;100: 15178–15183.
10 Galli R, Binda E, Orfanelli U et al. Isolation and characterization of tumorigenic, stem-like neural precursors from human glioblastoma. Cancer Res 2004;64:7011–7021.
11 Holland EC, Hively WP, DePinho RA et al. A constitutively active epidermal growth factor receptor cooperates with disruption of G1 cell-cycle arrest pathways to induce glioma-like lesions in mice. Genes Dev 1998;12:3675–3685.
12 Dai C, Celestino JC, Okada Y et al. PDGF autocrine stimulation dedifferentiates cultured astrocytes and induces oligodendrogliomas and oligoastrocytomas from neural progenitors and astrocytes in vivo. Genes Dev 2001;15:1913–1925.
13 Gilbertson RJ, Rich JN. Making a tumour's bed: Glioblastoma stem cells and the vascular niche. Nat Rev Cancer 2007;7:733–736.
14 Bao S, Wu Q, McLendon RE et al. Glioma stem cells promote radioresistance by preferential activation of the DNA damage response. Nature 2006;444:756–760.
15 Lee J, Elkahloun AG, Messina SA et al. Cellular and genetic characterization of human adult bone marrow-derived neural stem-like cells: A potential antiglioma cellular vector. Cancer Res 2003;63: 8877–8889.
16 Ailles LE, Weissman IL. Cancer stem cells in solid tumors. Curr Opin Biotechnol 2007;18:460–466.
17 Lee J, Son MJ, Woolard K et al. Epigenetic-mediated dysfunction of the bone morphogenetic protein pathway inhibits differentiation of glioblastoma-initiating cells. Cancer Cell 2008;13:69–80.
18 Piccirillo SG, Vescovi AL. Brain tumour stem cells: Possibilities of new therapeutic strategies. Expert Opin Biol Ther 2007;7: 1129–1135.
19 Marin-Husstege M, Muggironi M, Liu A et al. Histone deacetylase activity is necessary for oligodendrocyte lineage progression. J Neurosci 2002;22:10333–10345.
20 Hsieh J, Nakashima K, Kuwabara T et al. Histone deacetylase inhibition-mediated neuronal differentiation of multipotent adult neural progenitor cells. Proc Natl Acad Sci USA 2004;101: 16659–16664.
21 Kondo T, Raff M. Chromatin remodeling and histone modification in the conversion of oligodendrocyte precursors to neural stem cells. Genes Dev 2004;18:2963–2972.
22 de Ruijter AJ, van Gennip AH, Caron HN et al. Histone deacetylases (HDACs): Characterization of the classical HDAC family. Biochem J 2003;370:737–749.
23 Thiagalingam S, Cheng KH, Lee HJ et al. Histone deacetylases: Unique players in shaping the epigenetic histone code. Ann N Y Acad Sci 2003;983:84–100.
24 Peterson CL, Laniel MA. Histones and histone modifications. Curr Biol 2004;14:R546–R551.
25 Romanski A, Bacic B, Bug G et al. Use of a novel histone deacetylase inhibitor to induce apoptosis in cell lines of acute lymphoblastic leukemia. Haematologica 2004;89:419–426.
26 Balasubramaniyan V, Boddeke E, Bakels R et al. Effects of histone deacetylation inhibition on neuronal differentiation of embryonic mouse neural stem cells. Neuroscience 2006;143:939–951.
27 Prozorovski T, Schulze-Topphoff U, Glumm R et al. Sirt1 contributes critically to the redox-dependent fate of neural progenitors. Nat Cell Biol 2008;10:385–394.
28 Johnstone RW. Histone-deacetylase inhibitors: Novel drugs for the treatment of cancer. Nat Rev Drug Discov 2002;1:287–299.
29 Bar EE, Chaudhry A, Lin A et al. Cyclopamine-mediated hedgehog pathway inhibition depletes stem-like cancer cells in glioblastoma. Stem Cells 2007;25:2524–2533.
30 Vescovi AL, Parati EA, Gritti A et al. Isolation and cloning of multipotential stem cells from the embryonic human CNS and establishment of transplantable human neural stem cell lines by epigenetic stimulation. Exp Neurol 1999;156:71–83.
31 Eiraku M, Tohgo A, Ono K et al. DNER acts as a neuron-specific Notch ligand during Bergmann glial development. Nat Neurosci 2005; 8:873–880.
32 Reznik TE, Sang Y, Ma Y et al. Transcription-dependent epidermal growth factor receptor activation by hepatocyte growth factor. Mol Cancer Res 2008;6:139–150.
33 Towbin H, Staehelin T, Gordon J. Electrophoretic transfer of proteins from polyacrylamide gels to nitrocellulose sheets: Procedure and some applications. Proc Natl Acad Sci USA 1979;76:4350–4354.
34 Xia S, Rosen EM, Laterra J. Sensitization of glioma cells to Fas-dependent apoptosis by chemotherapy-induced oxidative stress. Cancer Res 2005;65:5248–5255.
35 Canes D, Chiang GJ, Billmeyer BR et al. Histone deacetylase inhibitors upregulate plakoglobin expression in bladder carcinoma cells and display antineoplastic activity in vitro and in vivo. Int J Cancer 2005; 113:841–848.
36 Lal B, Xia S, Abounader R et al. Targeting the c-Met pathway potentiates glioblastoma responses to gamma-radiation. Clin Cancer Res 2005;11:4479–4486.
37 Matsui W, Wang Q, Barber JP et al. Clonogenic multiple myeloma progenitors, stem cell properties, and drug resistance. Cancer Res 2008;68:190–197.
38 Kastan MB, Schlaffer E, Russo JE et al. Direct demonstration of elevated aldehyde dehydrogenase in human hematopoietic progenitor cells. Blood 1990;75:1947–1950.
39 Piccirillo SG, Reynolds BA, Zanetti N et al. Bone morphogenetic proteins inhibit the tumorigenic potential of human brain tumour-initiating cells. Nature 2006;444:761–765.
40 Cui XY, Hu QD, Tekaya M et al. NB-3/Notch1 pathway via Deltex1 promotes neural progenitor cell differentiation into oligodendrocytes. J Biol Chem 2004;279:25858–25865.
41 Yamamoto N, Yamamoto S, Inagaki F et al. Role of Deltex-1 as a transcriptional regulator downstream of the Notch receptor. J Biol Chem 2001;276:45031–45040.
42 Wu L, Sun T, Kobayashi K et al. Identification of a family of mastermind-like transcriptional coactivators for mammalian notch receptors. Mol Cell Biol 2002;22:7688–7700.
43 Stupp R, Mason WP, van den Bent MJ et al. Radiotherapy plus concomitant and adjuvant temozolomide for glioblastoma. N Engl J Med 2005;352:987–996.
44 Lindvall C, Bu W, Williams BO et al. Wnt signaling, stem cells, and the cellular origin of breast cancer. Stem Cell Rev 2007;3: 157–168.
45 Fan X, Matsui W, Khaki L et al. Notch pathway inhibition depletes stem-like cells and blocks engraftment in embryonal brain tumors. Cancer Res 2006;66:7445–7452.
46 Lyssiotis CA, Walker J, Wu C et al. Inhibition of histone deacetylase activity induces developmental plasticity in oligodendrocyte precursor cells. Proc Natl Acad Sci USA 2007;104:14982–14987.
47 Dalgard CL, Van Quill KR, O'Brien JM. Evaluation of the in vitro and in vivo antitumor activity of histone deacetylase inhibitors for the therapy of retinoblastoma. Clin Cancer Res 2008;14:3113–3123.
48 Saito A, Yamashita T, Mariko Y et al. A synthetic inhibitor of histone deacetylase, MS-27–275, with marked in vivo antitumor activity against human tumors. Proc Natl Acad Sci USA 1999;96:4592–4597.
49 Hahn CK, Ross KN, Warrington IM et al. Expression-based screening identifies the combination of histone deacetylase inhibitors and retinoids for neuroblastoma differentiation. Proc Natl Acad Sci USA 2008;105:9751–9756.
50 Camphausen K, Burgan W, Cerra M et al. Enhanced radiation-induced cell killing and prolongation of gammaH2AX foci expression by the histone deacetylase inhibitor MS-275. Cancer Res 2004;64: 316–321.
51 Simonini MV, Camargo LM, Dong E et al. The benzamide MS-275 is a potent, long-lasting brain region-selective inhibitor of histone deacetylases. Proc Natl Acad Sci USA 2006;103:1587–1592.
52 Eiraku M, Hirata Y, Takeshima H et al. Delta/Notch-like epidermal growth factor (EGF)-related receptor, a novel EGF-like repeat-

containing protein targeted to dendrites of developing and adult central nervous system neurons. J Biol Chem 2002;277:25400–25407.
53 Radtke F, Raj K. The role of Notch in tumorigenesis: Oncogene or tumour suppressor? Nat Rev Cancer 2003;3:756–767.
54 Artavanis-Tsakonas S, Rand MD, Lake RJ. Notch signaling: Cell fate control and signal integration in development. Science 1999;284:770–776.
55 Androutsellis-Theotokis A, Leker RR, Soldner F et al. Notch signalling regulates stem cell numbers in vitro and in vivo. Nature 2006;442:823–826.
56 Kanamori M, Kawaguchi T, Nigro JM et al. Contribution of Notch signaling activation to human glioblastoma multiforme. J Neurosurg 2007;106:417–427.
57 Hulleman E, Quarto M, Vernell R et al. A role for the transcription factor HEY1 in glioblastoma. J Cell Mol Med 2009;13:136–146.

See www.StemCells.com for supporting information available online.